

A Fundamental Equation of State for Heavy Water

Cite as: Journal of Physical and Chemical Reference Data **11**, 1 (1982); <https://doi.org/10.1063/1.555661>
Published Online: 15 October 2009

P. G. Hill, R. D. Chris MacMillan, and V. Lee



View Online



Export Citation

ARTICLES YOU MAY BE INTERESTED IN

[Erratum: Thermophysical Properties of Fluids. I. Argon, Ethylene, Parahydrogen, Nitrogen, Nitrogen Trifluoride, and Oxygen](#)

Journal of Physical and Chemical Reference Data **14**, 619 (1985); <https://doi.org/10.1063/1.555731>

[Erratum: A Fundamental Equation of State for Heavy Water \[J. Phys. Chem. Ref. Data 11, 1 \(1982\)\]](#)

Journal of Physical and Chemical Reference Data **12**, 1065 (1983); <https://doi.org/10.1063/1.555696>

[New International Formulations for the Thermodynamic Properties of Light and Heavy Water](#)

Journal of Physical and Chemical Reference Data **15**, 305 (1986); <https://doi.org/10.1063/1.555772>



Where in the **world** is AIP Publishing?
Find out where we are exhibiting next

A Fundamental Equation of State for Heavy Water

P. G. Hill, R. D. Chris MacMillan, and V. Lee

Department of Mechanical Engineering, The University of British Columbia, Vancouver, B. C. V6T 1W5

A fundamental equation of state has been formulated for heavy water in the form

$$\Psi = \Psi(\rho, T)$$

in which Ψ = Helmholtz free energy

ρ = density

T = thermodynamic temperature

The complete range of single phase states in the range up to 100 MPa and 600 °C is covered by a single equation which is fitted both to *PVT* values, for saturated and unsaturated states, and to enthalpy values for saturation states only. The equation is constrained to fit the critical point conditions determined by Blank. It represents all thermodynamic properties of D₂O, in the above range of states.

Key words: equation of state; enthalpy; Helmholtz function; heavy water; *PVT*; specific heats; speed of sound; thermodynamic properties; vapor pressure

Contents

	Page
1. Introduction	2
2. The Equation of State	2
3. The Fitting Procedure	4
4. The Data Base	4
4.1. The Ideal Gas States	4
4.2. Virial Coefficients	5
4.3. Joule-Thomson Coefficients	5
4.4. Vapor Pressure	5
4.5. <i>PVT</i> Data	6
4.6. Saturation States	7
4.7. Specific Heats	7
5. Constraints	7
5.1. Critical Conditions	8
5.2. Triple Point	8
5.3. Maximum Density Point	8
6. The Temperature Scale	8
7. <i>PVT</i> Data	8
7.1. Line of Maximum Density	9
7.2. Vapor Pressure Equation	9
7.3. Virial Coefficients	10
7.4. Specific Heats at Constant Pressure	10
7.5. Specific Heats at Constant Volume	10
7.6. Speed of Sound	11
7.7. Joule-Thomson Coefficients	12
8. Conclusion	12
Acknowledgment	13
References	13
Appendix A—Evaluation of C_1 and C_2	14

	Page
Figure 1. Distribution of $\Psi/P(\partial\Psi/\partial v)$ for D ₂ O liquid states	4
Figure 2. Specific heat of D ₂ O at low pressure	5
Figure 3. D ₂ O <i>PVT</i> data sources	5
Figure 4. Liquid saturation volumes: comparison of values	7
Figure 5. Vapor saturation volumes: comparison of values	7
Figure 6. Pressures at 200 °C: comparison of values ..	7
Figure 7. Pressures at 300 °C: comparison of values ..	7
Figure 8. Pressures at 371 °C and 375 °C: comparison of values	8
Figure 9. Pressures at 400 °C: comparison of values ..	8
Figure 10. Pressures at 500 °C: comparison of values ..	8
Figure 11. Volumes at 20 °C: comparison of values	8
Figure 12. Volumes at 40 °C: comparison of values	9
Figure 13. Volumes at 50 °C: comparison of values	9
Figure 14. Volumes at 150 °C: comparison of values	9
Figure 15. Volumes at 0.1 MPa: comparison of values ..	9
Figure 16. Line of maximum density calculated from Ψ equation	10
Figure 17. Saturation vapor pressure calculated from Ψ equation	10
Figure 18. Virial coefficients: comparison of values: 100–500 °C	10
Figure 19. Specific heats at constant pressure: 320–360 °C	10
Figure 20. Specific heats at constant pressure: 100–300 °C	11
Figure 21. Specific heats at constant pressure: 14.7, 17.2, 19.6 MPa	11
Figure 22. Specific heats at constant pressure: 22.1,	

© 1982 by the U.S. Secretary of Commerce on behalf of the United States. This copyright is assigned to the American Institute of Physics and the American Chemical Society.

Reprints available from ACS; see Reprint List at back of issue.

	23.5, 24.5 MPa	11	Figure 26. Speed of sound: comparison of values, 0–100 °C.....	12
Figure 23. Specific heats at constant pressure: 25.5, 27.0, 29.4 MPa		11	Figure 27. Speed of sound: comparison of values, 150–371 °C.....	12
Figure 24. Specific heats at constant volume: 0.9–1.1 cm ³ /g.....		12	Figure 28. Joule-Thomson coefficients: comparison of values, 130–170 °C	13
Figure 25. Specific heats at constant volume: 1.2–2.9 cm ³ /g.....		12		

1. Introduction

This paper describes the development of a fundamental equation for heavy water. The equation has the form

$$\Psi = \Psi(\rho, T)$$

in which Ψ is the specific Helmholtz free energy, ρ is the density, and T is the thermodynamic temperature. The equation represents a continuity of single phase states covering both liquid and vapor regions to about 100 MPa in pressure and 600 °C in temperature. From this equation all thermodynamic properties can be derived, including the saturation properties, within the experimental uncertainty.

It is only in recent years that sufficient data on the thermodynamic properties of D₂O have been acquired to permit a comprehensive formulation of this type. Vapor pressure data can now be said to be plentiful and the uncertainty in the vapor pressure is now less than 0.1%, except at low temperatures. *PVT* data for liquid states are also relatively abundant, but uncertainties in isotopic content mean that liquid volumes are not generally known within 0.01%, even at low temperatures. Experimentally determined virial coefficients are now available as well as critical-region and supercritical-region *PVT* data.

Considerable uncertainty still attaches to determination of saturation volumes (particularly on the vapor side at relatively high subcritical temperatures), and to determination of saturation enthalpies. Critical point parameters are also uncertain. The range of disagreement between reported values is as large as 1 °C, 0.1 MPa and 0.2 cm³/g, though Blank's determination of the critical temperature (by meniscus observation) differs by not more than 0.1 °C from the critical temperature one would infer from the critical region *PVT* data of Rivkin.

With these uncertainties in mind, it is clear that the accuracy of the best heavy water equation which it is possible to formulate at the present time will be less than that of existing light water equations of this type (see Keenan, Keyes, Hill and Moore[1]¹ and Pollak [2]). However the level of accuracy now attainable will be, in almost all respects, well within engineering requirements.

Previous tables and equations of state for D₂O properties are described in Kirschenbaum [3], Kesselman [4], Baker [5], Mamedov [6], Plank [7], Suvorov [8], Elliot [9], Kirrillin [10], Lundquist and Persson [11], Rosta [12], Ivey and Tarasuk [13], Scheffler, Nitsche and Straub [14], Ikeda, Kageyama, and Nagashima [15], and Juza and Mares [16]. A comprehensive bibliography of papers on D₂O has been compiled by Uematsu and Watanabe [17].

The great advantage of the fundamental equation formulation is that it guarantees complete consistency of *PVT* and ener-

gy, enthalpy, and entropy calculations. Moreover it contains the vapor pressure relationship (when used in conjunction with the two-phase equilibrium requirement). The equation also provides a calculation of all other thermodynamic variables including virial coefficients, Joule-Thomson coefficient, compressibility, and speed of sound. In principle all of the existing data on these variables can be used in the formulation process. The great contribution of high speed computing to the formulation process is in the possibility of fitting a single equation over the entire range of liquid and vapor states and over all kinds of available data. In practice, of course, it is wise to be selective, to include the highest quality data with appropriate weight, rather than including all data indiscriminately. Although experimental *PVT* measurements are now available to cover a broad temperature and pressure range, saturation values of liquid volume (v_l), vapor volume (v_g), liquid enthalpy (h_l), vapor enthalpy (h_g), and saturation pressure have been determined before the global fitting process begins. Previous papers (Hill and MacMillan [18] and [19]), describe a new vapor pressure formulation and the determination of saturation properties of D₂O.

2. The Equation of State

The equation of state has the following form:

$$\Psi = \Psi_0(T) + RT [\ln \rho + \rho Q(\rho, T)] \quad (1)$$

in which

$$Q = (\tau - \tau_c) \sum_{j=1}^7 (\tau - \tau_{aj})^{j-2} \left[\sum_{i=1}^8 A_{ij} (\rho - \rho_{aj})^{i-1} + e^{-E\rho} \sum_{i=9}^{10} A_{ij} \rho^{i-9} \right] \quad (2)$$

and

$$\Psi_0(T) = \sum_{i=1}^6 C_i \left(\frac{T}{1000} \right)^{i-1} + C_7 \ln T + \frac{C_8 T \ln T}{1000} \quad (3)$$

$$R = 0.41515 \text{ kJ/kg K.}$$

The units are as follows:

Ψ, Ψ_0	Specific Helmholtz free energy, kJ/kg
T	Absolute thermodynamic temperature, K
τ	$1000/T, \text{K}^{-1}$
ρ	Density, 10^3kg/m^3 , i.e., g/cm ³

The constants in the double series expansion of Q are:

τ_c	= 1.553	E	= 4.3
τ_{aj}	= 1.553	($j=1$)	ρ_{aj} = 0.7 ($j=1$)
τ_{aj}	= 2.53	($j>1$)	ρ_{aj} = 1.1 ($j>1$)

¹Figures in brackets indicate literature references at the end of this paper.

The coefficients C_j are given as follows:

$$\begin{aligned} C_1 &= 1866.81 & C_5 &= 100.1333 \\ C_2 &= 4661.5 & C_6 &= -13.135 \\ C_3 &= 64.605 & C_7 &= 0.32684 \\ C_4 &= -284.8833 & C_8 &= -1211.253 \end{aligned}$$

and the coefficients A_{ij} are given in table 1. The coefficients C_1 and C_2 have been chosen so that the internal energy and Helmholtz free energy are both zero in the triple point liquid state, as shown in Appendix A.

From the fundamental equation the following properties are obtained by differentiation:

Pressure:

MPa

$$\begin{aligned} P &= \rho^2 \left(\frac{\partial \Psi}{\partial \rho} \right)_\tau \\ P &= \rho RT \left[1 + \rho Q + \rho^2 \left(\frac{\partial Q}{\partial \rho} \right)_\tau \right] \end{aligned} \quad (4)$$

Specific Internal Energy:

$$\begin{aligned} &\text{kJ/kg} \\ u &= \left[\frac{\partial (\Psi \tau)}{\partial \tau} \right]_\rho \\ u &= \frac{d}{d\tau} (\Psi_0 \tau) + RT \rho \tau \left(\frac{\partial Q}{\partial \tau} \right)_\rho \end{aligned} \quad (5)$$

TABLE 1. The coefficients A_{ij}

i	j	A_{ij}	i	j	A_{ij}
1	1	73.13848592	1	5	-6.73408249
2	1	-285.20415917	2	5	24.03602093
3	1	535.71659288	3	5	-41.08079830
4	1	-649.81000614	4	5	45.39111005
5	1	574.63280680	9	5	139.21659329
6	1	-387.92157774	10	5	566.02305152
7	1	206.34569512	1	6	-5.24802962
8	1	-79.89428513	2	6	18.52690633
9	1	-996.36169097	3	6	-31.42397369
10	1	-766.27290006	4	6	26.43208802
1	2	24.74108348	9	6	96.31411481
2	2	-105.57317181	10	6	453.20280933
3	2	200.87302906	1	7	-1.17583447
4	2	-235.18776440	2	7	4.13816432
5	2	224.56976938	3	7	-6.55842224
6	2	-40.09924297	4	7	4.75774631
7	2	128.77154771	9	7	19.39184297
8	2	-28.40907978	10	7	103.56819758
9	2	-1389.08003142			
10	2	-1672.09705556			
1	3	11.64775625			
2	3	-42.51820251			
3	3	72.45541064			
4	3	-82.55391089			
9	3	-267.85482520			
10	3	-998.64982710			
1	4	2.66566642			
2	4	-9.19657655			
3	4	15.13096920			
4	4	-7.24860975			
9	4	-46.83904320			
10	4	-227.34793319			

Specific Entropy:

$$\begin{aligned} &\text{kJ/kg K} \\ s &= - \left(\frac{\partial \Psi}{\partial T} \right)_\rho \\ s &= -R \left[\ln \rho + \rho Q + \rho T \frac{\partial Q}{\partial T} \right] - \frac{d\psi_0}{dT} \end{aligned} \quad (6)$$

Specific Enthalpy:

$$\begin{aligned} &\text{kJ/kg} \\ h &= u + P/\rho \\ h &= RT \left[1 + \rho Q - \rho T \frac{\partial Q}{\partial T} + \rho^2 \frac{\partial Q}{\partial \rho} \right] + \frac{d(\psi_0 \tau)}{d\tau} \end{aligned} \quad (7)$$

Other properties are obtained as follows:

Specific Heats:

$$\begin{aligned} &\text{kJ/kg K} \\ C_p &= \left(\frac{\partial h}{\partial T} \right)_\rho \\ C_p &= \left(\frac{\partial h}{\partial T} \right)_\rho - \frac{\left(\frac{\partial h}{\partial \rho} \right)_\tau \left(\frac{\partial P}{\partial T} \right)_\rho}{\left(\frac{\partial P}{\partial \rho} \right)_\tau} \\ C_v &= \left(\frac{\partial u}{\partial T} \right)_\rho \end{aligned} \quad (8)$$

Second Virial Coefficient:

$$\begin{aligned} &(10^3 \text{kg/m}^3)^{-1} \\ B &= (Q)_{\rho \rightarrow 0} \end{aligned} \quad (9)$$

Third Virial Coefficient:

$$\begin{aligned} &(10^3 \text{kg/m}^3)^{-2} \\ C &= \left(\frac{\partial Q}{\partial \rho} \right)_{\rho \rightarrow 0} \end{aligned} \quad (10)$$

Joule-Thomson Coefficient:

$$\begin{aligned} &\text{K/MPa} \\ \mu &= \left(\frac{\partial T}{\partial P} \right)_h \\ \mu &= - \left(\frac{\partial h}{\partial P} \right)_T \frac{1}{C_p} = \frac{1}{\rho C_p} \left[T \left(\frac{\partial P}{\partial T} \right)_\rho - 1 \right] \end{aligned} \quad (11)$$

Compressibility (Isothermal):

$$\begin{aligned} &(\text{MPa})^{-1} \\ K_T &= \left[\rho \left(\frac{\partial P}{\partial \rho} \right)_T \right]^{-1} \end{aligned} \quad (12)$$

Speed of Sound:

$$\begin{aligned} &\text{m/s} \\ a &= \left[\frac{1}{\left(\frac{\partial P}{\partial \rho} \right)_T} - \frac{T}{C_p \rho^2} \left(\frac{\partial P}{\partial T} \right)_\rho \right]^{-1/2} \end{aligned} \quad (13)$$

The vapor pressure is obtained from the equation of state by satisfying the condition

$$(\Psi + P/\rho)_v = (\Psi + P/\rho)_g, \quad (14)$$

where *f* and *g* denote the saturated liquid and vapor phases, respectively.

3. The Fitting Procedure

The fitting procedure determines the coefficients A_{ij} by minimizing the quantity

$$D = \sum_{i=1}^N \left[\frac{P_{\text{obs}} - P_{\text{calc}}}{\Delta P} \right]^2 + \sum_{i=1}^M \left[\frac{h_{\text{obs}} - h_{\text{calc}}}{\Delta h} \right]^2 + \sum_{i=1}^K \left[\frac{\zeta_g - \zeta_f}{\Delta \zeta} \right]^2 + \sum_{i=1}^L \lambda_i G_i \quad (15)$$

in which the first summation includes all *PVT* data points included in the fitting procedure and the second summation includes the enthalpy data points. The subscripts "obs" and "calc" refer to data points and calculated values, respectively. The third summation includes a weighted least squares fit to the saturation equilibrium condition (ζ_f and ζ_g being the chemical potential of saturated liquid and saturated vapor, respectively). This summation extends over a number (about 20) of the subcritical isotherms. The coefficients λ_i in the fourth summation are the Lagrange multipliers corresponding to the constraints G_i .

The terms ΔP , Δh and $\Delta \zeta$, which provide the weighting for the least squares summations, are the r.m.s. uncertainties of the dependent variable for each data point. For the *PVT* data

$$\frac{\Delta P}{P} = \left[\left(\frac{\delta P}{P} \right)^2 + \left(\frac{V}{P} \frac{\partial P}{\partial V} \frac{\delta V}{V} \right)^2 + \left(\frac{T}{P} \frac{\partial P}{\partial T} \frac{\delta T}{T} \right)^2 \right]^{1/2} \quad (16)$$

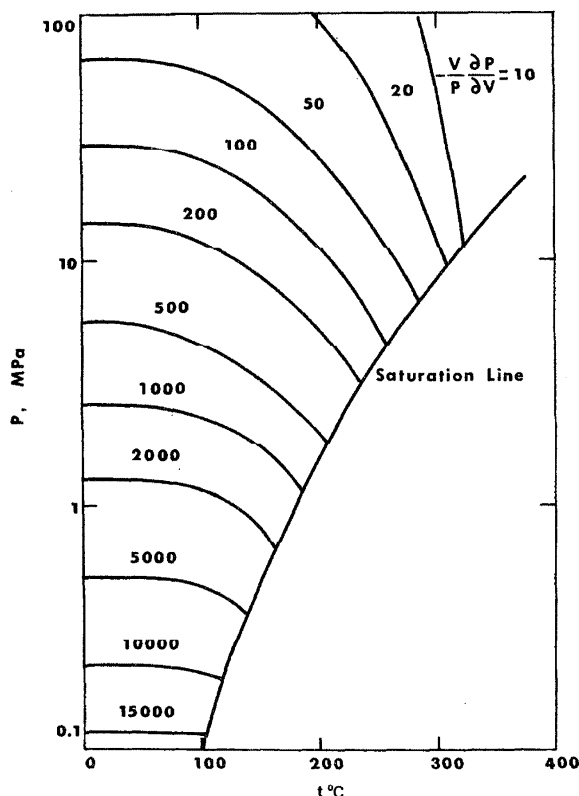


FIGURE 1. $(V/P)(\partial P/\partial V)$ for D_2O liquid states.

in which δP , δV and δT are the experimental uncertainties in pressure, volume, and temperature measurements, respectively. Nominal values, corresponding to best experimental technique are

$$\begin{aligned} \frac{\delta P}{P} &= 10^{-3}, \\ \frac{\delta V}{V} &= 10^{-4}, \\ \frac{\delta T}{T} &= 2 \times 10^{-5} \text{ to } 5 \times 10^{-5}. \end{aligned}$$

With H_2O data $\delta P/P$ and $\delta V/V$ can be as low as 10^{-4} and 10^{-5} , respectively, but for D_2O measurements the effect of H_2O and other isotopic content (with some uncertainty in composition) means that $\delta P/P$ and $\delta V/V$ are an order of magnitude larger even after attempts are made to correct the isotopic content. With the difference in specific volumes of H_2O and D_2O of the order of 10% and the uncertainty of actual H_2O content in experimental samples approaching 0.1%, the volume uncertainty is of the order of 10^{-4} .

The evaluation of ΔP with eq (16) depends strongly on the term $V/P \partial P/\partial V$ which reaches large values for low temperature liquid states. Figure 1 indicates the variation of this parameter throughout the liquid region as determined by the resulting equation of state for D_2O . With the previously stated values for $\delta P/P$, $\delta V/V$, $\delta T/T$, the dominant contribution to ΔP will come from the volume term, for $V/P \partial P/\partial V > 10$, i.e., for virtually all of the compressed liquid states. For low temperature liquid states

$$\Delta P \approx V \frac{\partial P}{\partial V} \frac{\delta V}{V} = \frac{-1}{K_T} \frac{\delta V}{V}$$

in which K_T is the compressibility, and is of the order of 10^{-4} bar $^{-1}$. This means that ΔP will nominally be of the order of 1 bar in the low temperature liquid region. The values for ΔP are set with reference to eq (16) and any evidence of systematic errors are revealed by incompatibilities between overlapping data sets. For the vapor states the terms $V/P \partial P/\partial V$ and $T/P \partial P/\partial T$ are small enough that the dominant contribution to $\Delta P/P$ is the term $\delta P/P$ which means that $\Delta P/P$ is of the order 10^{-3} (a value of 2×10^{-3} is generally used for specific volumes greater than $1.4 \text{ cm}^3/\text{g}$).

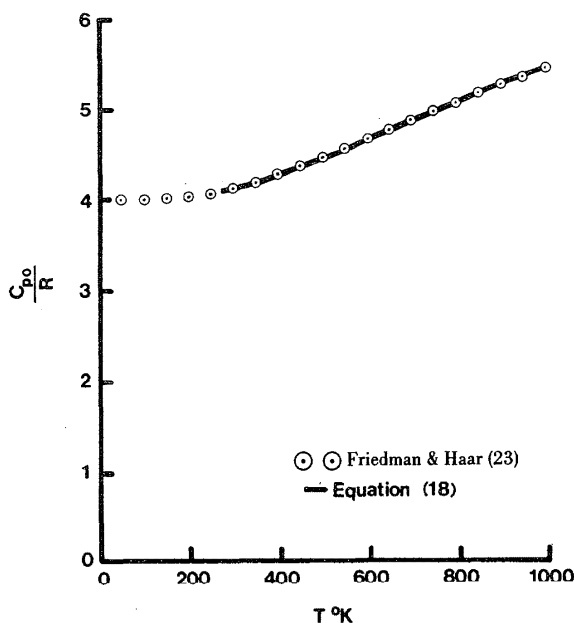
For the second summation in eq (15), only the enthalpy values for liquid saturation states have been used. The nominal uncertainty of the saturated liquid enthalpies has been taken as proportional to the enthalpy; it is 0 at the triple point and 2 J/g at 300 °C.

Determination of the coefficients A_{ij} by a least squares procedure, subject to a number of fixed constraints which are specified in section 5, follows a standard procedure (see McCarty [20]) except that the adjustment of the expansion points (ρ_{aj} , τ_{aj}), and use of high precision arithmetic are necessary to assure successful matrix inversion.

4. The Data Base

4.1. The Ideal Gas States

The molecular weight of 100 per cent D_2O (with the same relative abundance of oxygen isotopes as in standard mean ocean water) is given by Kell [21] as 20.027048. The difference

FIGURE 2. Specific heat of D₂O at low pressure.

between this value and the value 20.0284 (International Atomic Weights 1955) used by Whalley [22] and others will have negligible effect on the fitting process. The corresponding gas constant is 8.31434 kJ/(kg mol K) or 0.41515 kJ/(kg K).

Specific heat values are provided by Friedman and Haar [23] for the temperature range 50–5000 K. Figure 2 shows their values of specific heat of D₂O in the range of 270–1250 K in comparison with the following derivation from eq (1) for $\rho \rightarrow 0$.

$$\frac{C_{po}}{R} = \sum_{i=1}^6 \frac{C_i(2-i)(i-1)}{RT} \left(\frac{T}{1000}\right)^{i-1} + \frac{C_7}{RT} + 1 - \frac{C_8}{1000R} \quad (17)$$

in which C_i values are given under eq (3). This equation fits the values of Friedman and Haar within 0.05%.

The corresponding zero pressure enthalpy equation is

$$h_o = \sum_{i=1}^6 \frac{C_i(2-i)T^{i-1}}{1000^{i-1}} + C_7(\ln T - 1) + \left[R - \frac{C_8}{1000}\right]T \quad (18)$$

TABLE 2. Differences between second virial coefficients of H₂O and D₂O

t (°C)	$B_{H_2O} - B_{D_2O}$ Kell, McLaurin & Whalley [24]	cm^3/mol McLaurin & Kell [25]
150		0.60
200	3	0.41
225	2.8	0.35
250	1.1	0.30
275	0.77	0.27
300	0.70	0.24
325	0.38	
350	0.22	
375	0	
400	0.08	
425	0.03	
450	0.05	

4.2. Virial Coefficients

Values of the second and third virial coefficients of D₂O have been provided by Kell, McLaurin and Whalley [24]; table 2 provides the differences $B_{H_2O} - B_{D_2O}$ obtained in their paper.

Recent data of Kell [25] on the vapor volumes of both H₂O and D₂O in the range 150–350° permit direct determination of the differences between the second virial coefficients. The method and the results of these calculations are provided in reference [26]; table 2 indicates that these differences are small, of the order of 0.2% of the second virial coefficient for D₂O.

4.3. Joule-Thomson Coefficients

The main indication of gas imperfection for the low temperature vapor states is the Joule-Thomson coefficient data presented by Juza, Kmonicek, Sifner and Schovanec [27], which are limited to a small range of pressure and temperature.

4.4. Vapor Pressures

The vapor pressure of D₂O was formulated by Tanishita, Watanabe, Uematsu and Eguchi [28]. Since publication of their equation in 1974, no new data has appeared. However, in this work we rely on a new formulation (Hill and MacMillan [18]) which followed a reconsideration of unsmoothed experimental data. This proved to be particularly important for temperatures below 100 °C, the range in which smoothed data of various experimentalists show wide disagreement. Inspection of unsmoothed data was necessary to establish the apparent experimental uncertainty for each data set, after appropriate corrections had been made for H₂O concentration in the D₂O samples.

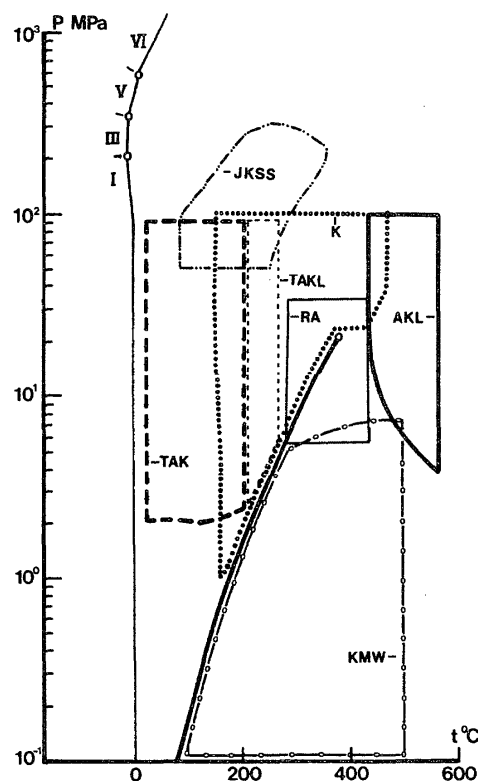
FIGURE 3. D₂O PVT data sources used in formulation. TAK: Tsederberg et al. (32); TAKL: Tsederberg et al. (33); JKSS: Juza et al. (27); K: Kell et al. (25); RA: Rivkin and Ahkundov (31); AKL: Alexandrov (35); KMW: Kell et al. (24).

TABLE 3. Sources of *PVT* data

Author	Ref	Data	Page/ table	Temp range (°C)	Press range (MPa)	Purity %
Rivkin & Akhundov	[31]	(1962)	62/2	275-425	5-34 ^a	99.87
Juza et al.	[27]	(1966)	369/3	80-350	50-350 ^b	99.86
Tsederberg et al.	[32]	(1972)	68/2	20-200	14-100	99.66
Tsederberg et al.	[33]	(1973)	14/1	200-425	2-100 ^a	99.8
Emmet & Millero	[34]	(1975)	352/2	2-40	0.1-100 ^a	> 99.8
Alexandrov et al.	[35]	(1976)	4/2	400-550	4-100	99.7- 99.8
Kell	[25]	(1979)	/1	150-450	.5-100	~100

^aSome data omitted (where isotherms are very close together).

^bData at 500 bar omitted.

The equation formulated is similar to the equations which Pollak [2] and Wagner [29] have shown to be successful in correlating H₂O vapor pressure data. The equation was developed using a statistical criterion for retaining only the most significant terms. It satisfies the critical point pressure and temperature determined by Blank [30], and also incorporates the critical point singularity

$$\frac{d^2P}{dT^2} \rightarrow (T_c - T)^{-\theta} \quad \theta = 0.1$$

The new D₂O vapor pressure equation is as follows:

$$\ln \frac{P}{P_c} = \frac{T_c}{T} (\alpha_1 \tau + \alpha_2 \tau^{1.9} + \alpha_4 \tau^2 + \alpha_{11} \tau^{5.5} + \alpha_{20} \tau^{10}) \quad (19)$$

in which

$$\tau = 1 - \frac{T}{T_c}$$

$$T_c = 643.89 \text{ K (IPTS 68)}$$

$$P_c = 21.66 \text{ MPa}$$

and

$$\alpha_1 = -7.81583 \quad \alpha_{11} = -3.92488$$

$$\alpha_2 = 17.6012 \quad \alpha_{20} = 4.19174$$

$$\alpha_4 = -18.1747$$

4.5. *PVT* Data

The *PVT* data used in the fitting process were obtained from Rivkin and Akhundov [31], Juza, Kmonicek, Sifner and Scholvanec [27], Tsederberg, Alexandrov and Khasanshin [32], Tsederberg, Alexandrov, Khasanshin and Larkin [33], Emmet and Millero [34], Alexandrov, Khasanshin and Larkin [35], and Kell [25]. Some data on closely neighbouring isotherms were omitted, as were data for volumes greater than 0.010 m³/kg at subcritical temperatures. The tolerances were assumed to depend only on (*P*, *T*), not on the data set. The pressure and temperature ranges for these data are shown in figure 3.

Data omitted in the fitting process included the measurements of Bridgman [36], Rivkin [37], Kirillin and Ulybin [38], Rivkin and Akhundov [39], Steckel and Szapiro [40], Alexandrov, Khasanshin and Larkin [41], and various measurements at saturation and atmospheric pressure (see Kirillin [10], Uematsu and Watanabe [17] and Kell [42]).

In addition, Rivkin and Akhundov [31] and Kell [25] and Alexandrov et al. [35] adequately cover the region above 300 °C, and so the data of Tsederberg, Alexandrov, Khasanshin and Larkin [33] in that region were omitted.

All volumes were corrected to 100% D₂O using the following correction formula (which assumes zero "volume of mixing")

$$v_{D_2O} = \frac{v_{obs} - v_{H_2O} Y}{1 - Y}$$

in which v_{obs} is the observed specific volume, v_{H_2O} is the specific volume of H₂O at the same pressure and temperature and *Y* is the mass fraction of H₂O in the experimental sample. The quantity v_{H_2O} was determined by use of the equation of Keenan, Keyes, Hill and Moore [1]. In the region very near the critical, the results of this method of correction for H₂O impurity were found to differ somewhat from those of the method of Hastings, Levelt Sengers and Balfour [43] which utilizes the corresponding states principle. Given these differences, data in the region 362 < θ < 380 °C and 200 < ρ < 500 kg/m³ were excluded from the fitting process.

TABLE 4. Saturation States of D₂O

<i>t</i> °C (IPTS 68)	<i>P</i> _{sat} MPa	<i>v</i> _l cm ³ /g	<i>v</i> _g	<i>h</i> _l J/g	<i>h</i> _g
3.8	.000660	.90464	174115	0.0	2324.0
6.0	.000774	.90439	149645	9.3	2327.7
10.0	.001026	.90419	114461	26.4	2334.6
15.0	.001442	.90428	82893	47.4	2342.9
20.0	.001999	.90472	60818	68.6	2351.3
25.0	.002737	.90545	45175	89.8	2359.7
30.0	.003702	.90645	33949	110.8	2367.8
35.0	.004950	.90771	25796	131.8	2376.0
40.0	.006549	.90918	19807	152.8	2384.1
49.99	.011115	.91274	12030	194.7	2400.3
100.0	.096252	.94057	1585.8	404.0	2479.0
111.02	.141942	.94866	1102.1	450.1	2495.2
150.0	.465323	.98296	361.22	613.7	2546.3
200.0	1.546004	1.04354	114.87	825.0	2588.7
250.0	3.995293	1.13149	44.61	1046.8	2596.3
275.0	5.997285	1.19270	28.99	1167.5	2583.4
300.0	8.688479	1.2740	19.03		
325.0	12.267	1.3917	12.34		
350.127	16.845	1.6044	7.493		
360.057	19.028	1.7709	5.792		

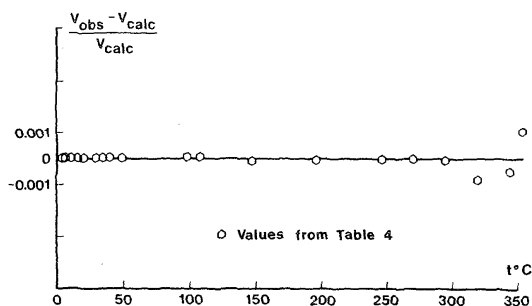


FIGURE 4. Liquid saturation volumes: comparison of values.

Values of percent D_2O composition are listed in table 3. A value of 99.87% was inferred for the Emmet and Millero data from comparison with the data of Steckel and Szapiro. Kell [42] indicates that the values of Steckel and Szapiro may be low by as much as $0.00003 \text{ cm}^3/\text{g}$ at 20°C , and cites recent atmospheric pressure measurements which differ by $\pm 0.00005 \text{ cm}^3/\text{g}$ from the data of Steckel and Szapiro at 20°C . (The value $0.9043546 \text{ cm}^3/\text{g}$ for 98.78% D_2O at 11.22°C_{46} was used to obtain absolute densities from the Steckel and Szapiro paper). Kell [42] considers that a standard D_2O sample has an oxygen isotopic composition identical to that of standard mean ocean water, and shows that control of oxygen isotope composition is necessary for accurate measurements.

Tsederberg et al. [32], [33] do not mention a temperature scale; the temperatures are assumed to be IPTS-48. The data of Emmet and Millero [34] are reported in "bars applied pressure"; one standard atmosphere (0.101325 MPa) is therefore added to these pressures. Where possible, unsmoothed data were used. The data of Juza et al. [27] are published in smoothed form only.

4.6. Saturation States

Hill and MacMillan [19] determined a set of saturation states for D_2O by extrapolating liquid volume and specific heat data and using a vapor virial equation and the Clapeyron equation. Table 4 presents a revision of this set of states, resulting from use of recent data and an improved calculation.

From 150°C to 325°C saturated liquid volumes have been determined from the recent measurements of Kell [25] of compressed liquid volumes.

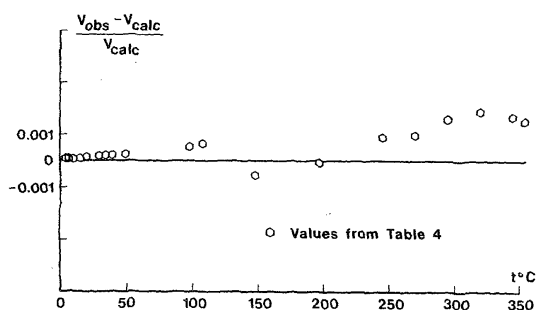
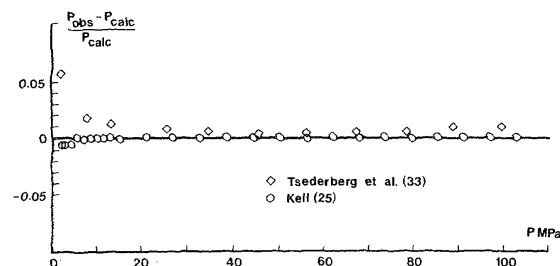


FIGURE 5. Vapor saturation volumes: comparison of values.

FIGURE 6. Pressures at 200°C : comparison of values.

The saturated vapor volumes up to 275°C have been recalculated after deriving new virial equations for H_2O and D_2O [26], using well known vapor data for H_2O and the recent Kell volume measurements for both H_2O and D_2O vapor.

Above 150°C the saturated liquid enthalpy values have been revised to be consistent with saturated vapor enthalpies (derived from the virial equation) and the saturated liquid and vapor volumes. From 3.8 to 150°C the saturated liquid enthalpies are the same as in [19], integrated from the triple point with extrapolated specific heat values (corrected for compressibility effect). In this temperature range the saturated vapor enthalpy values have been determined from the virial equation and the saturated vapor volumes have been adjusted for thermodynamic consistency with the h_g , h_f , and v_f values. From 200 to 275°C the saturated vapor enthalpies have been determined from the virial equation.

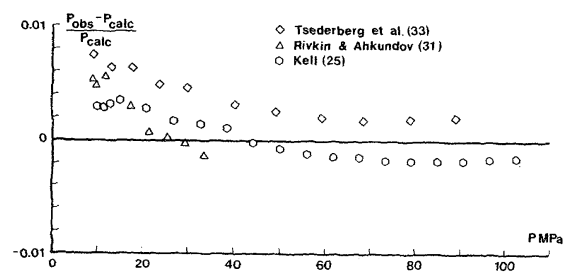
4.7. Specific Heats

Specific heats at constant pressure for D_2O have been reviewed by Rosta [12], who has analyzed the data of Rivkin and Egorov [44], [45], Cockett and Ferguson [46], and Eucken and Eigen [47].

Specific heats at constant volume for a number of isochores in the vicinity of the critical point have been reported by Amirkhanov, Stepanov and Mursalov [48].

5. Constraints

The following conditions are fixed in the least squares procedure by use of Lagrangian multipliers: triple point tempera-

FIGURE 7. Pressure at 300°C : comparison of values.

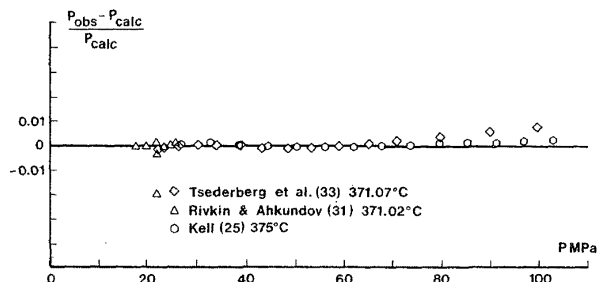


FIGURE 8. Pressures at 371/375 °C: comparison of values.

ture, pressure and energy, critical point temperature and volume, two values of the second virial coefficient B at high temperature, and one point along the line of maximum density. The introduction of a constraint requires the least squares equation to satisfy exactly the constraint condition.

5.1. Critical Conditions

The critical pressure and temperature above were determined by Blank [30]. This determination (unlike others in earlier literature) is in close agreement with the near critical isotherms of Rivkin and Ahkundov [31] (see reference [19]).

$$P_c = 21.66 \text{ MPa}$$

$$T_c = 370.66 \text{ °C (IPTS 48)}$$

$$= 370.74 \text{ °C (IPTS 68)}$$

$$\rho_c = 358 \text{ kg/m}^3$$

The critical pressure was not constrained in the fitting process but the first and second derivatives were set equal to zero. The critical pressure determined by the equation was 21.679 MPa, which agrees with the Blank value within what is believed to be the experimental uncertainty.

5.2. Triple Point

$$\text{At } \theta = 3.8 \text{ °C}_{48} = 3.8 \text{ °C}_{68}$$

and

$$\rho_f = 1.1054 \text{ g/cm}^3$$

we arbitrarily set

$$u_f = 0$$

$$\Psi_f = 0.$$

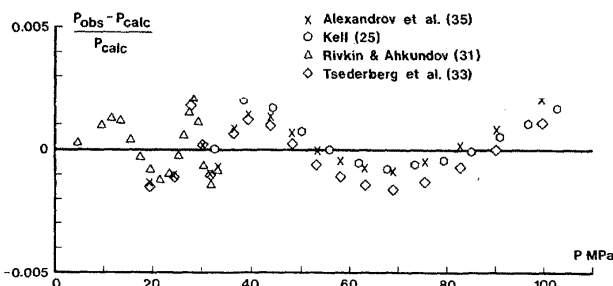


FIGURE 9. Pressures at 400 °C: comparison of values.

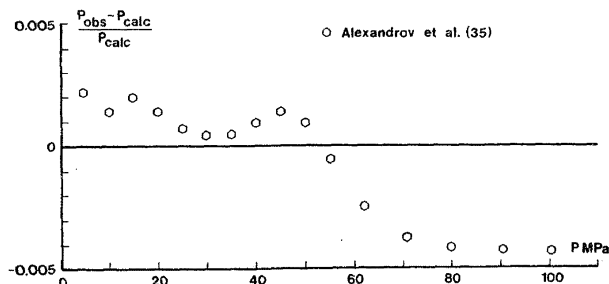


FIGURE 10. Pressures at 500 °C: comparison of values.

5.3. Maximum Density Point

$$\text{At } \theta = 11.2 \text{ °C}$$

and

$$\rho = 1.106 \text{ g/cm}^3$$

$$\left(\frac{\partial P}{\partial T}\right)_\rho = \left(\frac{\partial \rho}{\partial T}\right)_P = 0.$$

We also set

$$B = -0.75 \text{ cm}^3/\text{g} \quad \text{at } T = 840 \text{ °C (IPTS 68)}$$

$$B = 0 \quad \text{at } T = 1265.5 \text{ °C (IPTS 68)}.$$

6. The Temperature Scale

Data in which the temperatures are reported in IPTS 48 are converted to IPTS 68 using the equations given by Bedford and Kirby [49]. Between 0 °C and 630.74 °C we have

$$t_{68} = t_{48} + w(t) + z(t)$$

where t is the Celsius temperature, and

$$w(t) = 0.00045t(t/100 - 1) \times (t/419.58 - 1) \times (t/630.74 - 1)$$

and

$$z(t) = \frac{4.9035 \times 10^{-5} t(t/100 - 1)}{1 - 2.94855 \times 10^{-4} t}.$$

The arguments of w and z may be either t_{68} or t_{48} without loss of precision.

7. PVT Data

Figures 4 and 5 compare the saturation PVT values used as input to the fitting process (from table 4), and those calculated

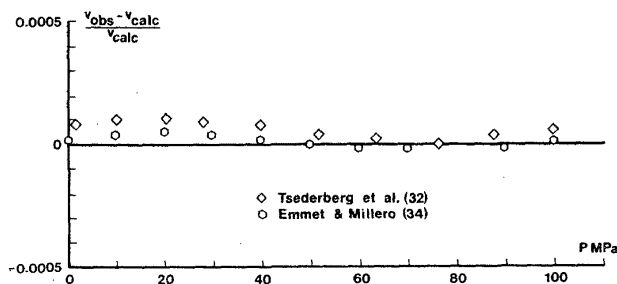


FIGURE 11. Volumes at 20 °C: comparison of values.

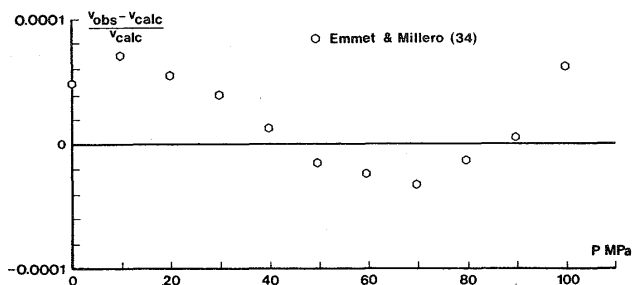


FIGURE 12. Volumes at 40 °C: comparison of values.

by the resulting equations. Figure 4 shows the differences below 300° between fitted and "data" values of saturated liquid volumes to be generally less than 1 in 10^4 , i.e., within experimental accuracy. Figure 5 indicates the discrepancy between the equation and the table 4 values of saturated vapor volumes to be less than 1 part in 10^3 up to 250 °C. At 325 °C extrapolations to saturation of existing vapor volumes are difficult so that the uncertainty in this volume is about 0.2%, i.e. about the same as the difference between the equation value and the one from table 4.

Figures 6, 7, 8, 9 and 10 show the comparisons between measured and calculated pressures. In figure 6 the agreement with the Kell [25] data is within 2% except for lower pressures where the volume uncertainty of 0.01% necessarily means a pressure uncertainty greater than 2%. Consider for example the large discrepancy with the Tsederberg data shown at 200 °C and 2 MPa (fig. 6), which is somewhat over 5%. Figure 1 would suggest that for these conditions

$$\frac{V}{P} \frac{\partial P}{\partial V} = 0 \quad (500)$$

so that a volume discrepancy of 0.01% could be equivalent to a pressure uncertainty of as much as 5%. In the light of this, figures 6 and 7 show good agreement between calculated and experimental pressures.

Figure 8 indicates close agreement with the Rivkin near-critical isotherm (371.02 °C₆₈, the critical temperature being taken to be 370.74 °C₆₈), but a large discrepancy with the Tsederberg data at high pressures. In this region the agreement with Kell [25] is within 0.27%.

At 400 °C, figure 9 indicates a close degree of agreement between Tsederberg et al. and Rivkin and Ahkundov data, and a fit to the equation of state within 0.2%. At these high tempera-

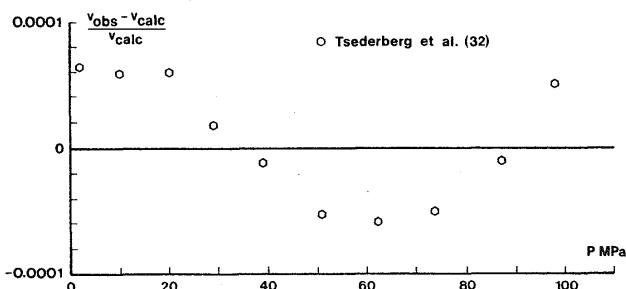


FIGURE 13. Volumes at 50 °C: comparison of values.

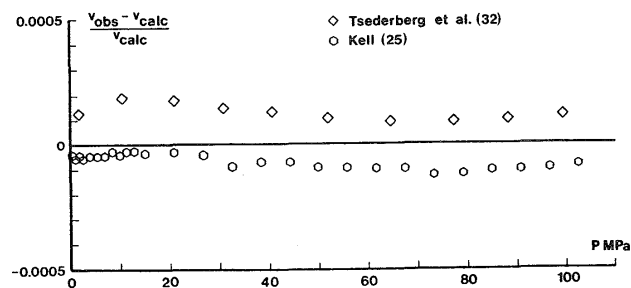


FIGURE 14. Volumes at 150 °C: comparison of values.

tures the effect of H₂O impurity corrections are not as significant as at lower temperatures.

Figure 10 shows that, at 500 °C, the equation differs from the data of Alexandrov, Khasanshin and Larkin [35] by as much as 0.4% at maximum pressure. This is the only data available in this region.

Figures 11, 12, 13 and 14 show volume discrepancies at lower temperatures. The discrepancies are within 0.01% except at 150 °C where the difference between Tsederberg and Kell data is about 0.02%.

At 70 °C, figure 15 shows the discrepancy between the equation and the 0.1 MPa data of Steckel and Szapiro (which were not used in the fitting process) to be less than 0.01%. The Steckel and Szapiro data were used to infer the purity of the Emmet and Millero data up to 40 °C.

7.1. Line of Maximum Density

Figure 16 compares the maximum density line calculated from the Ψ equation with the calculation of Alexandrov, Larkin, Matveev, Ershova [51] and the calculation of Alexandrov [52] from speed of sound data. It may be noted that the maximum density line was constrained to pass through 11.2 °C and 1.106 g/cm³.

7.2. Vapor Pressure Equation

Figure 17 shows the comparison between the vapor pressure calculated from the Helmholtz equation and eq (19) which is a direct fit to the vapor pressure data. As shown, the discrepancy is less than 0.02% except within 4 or 5 degrees of the critical point where the discrepancy rises to 0.05%, which is of the order of the uncertainty of the critical pressure of heavy water.

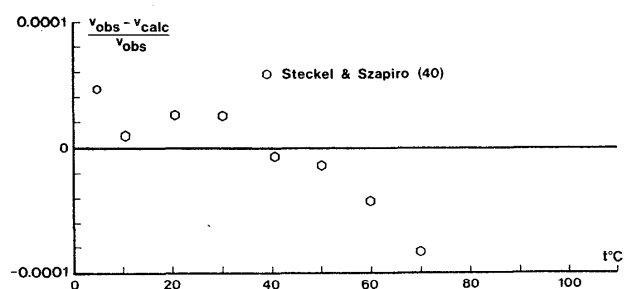
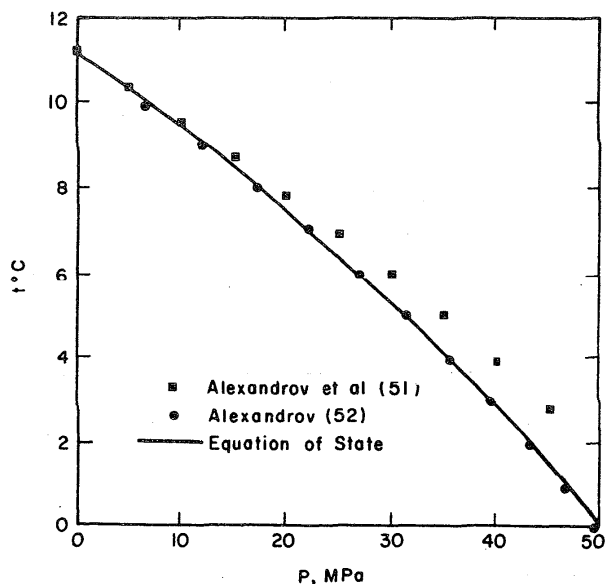


FIGURE 15. Volumes at 0.1 MPa: comparison of values.

FIGURE 16. Line of maximum density calculated from ψ equation.

7.3. Virial Coefficients

Figure 18 compares the virial coefficients calculated from the equation of state with the second virial coefficient of Kell, McLaurin and Whalley [24] and Kell [25].

7.4. Specific Heats at Constant Pressure

Figures 19, 20, 21, 22 and 23 indicate close agreement between the equation of state and the specific heat data of Rivkin and Egorov [44], [45], [53]. The agreement provides a strong check of the equation, since only the inferred saturation values of C_p were used in determining the liquid saturation line. None of the C_p values for the compressed liquid or superheated vapor states were included in the fit. Figures 22 and 23 show that the equation consistently underestimates the maximum value of C_p .

7.5. Specific Heats at Constant Volume

Figures 24 and 25 indicate reasonably good agreement between the equation and the experimental C_v values of Amirkhanov at low volumes, but a considerable discrepancy in the region of the critical volume ($v_c \approx 2.76$ cc/g). This discrepancy

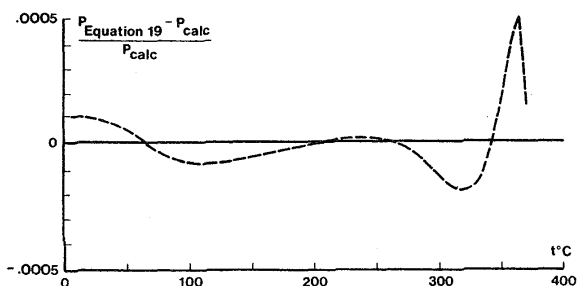
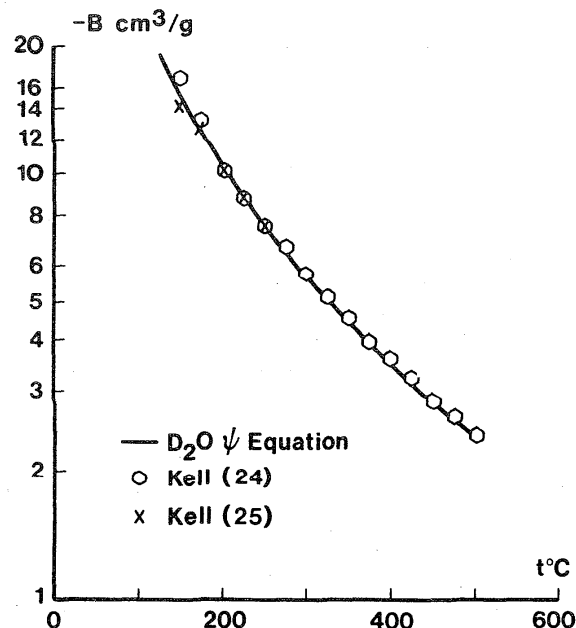
FIGURE 17. Saturation vapor pressure calculated from ψ equation.

FIGURE 18. Virial coefficients: comparison of values 100–500 °C.

may be due to the attempt to use an analytic equation to represent the non-analytic character of the critical region. The analytic equation will show C_p undergoing a step change at the critical isochore, in crossing the saturation line. Non-analytic critical

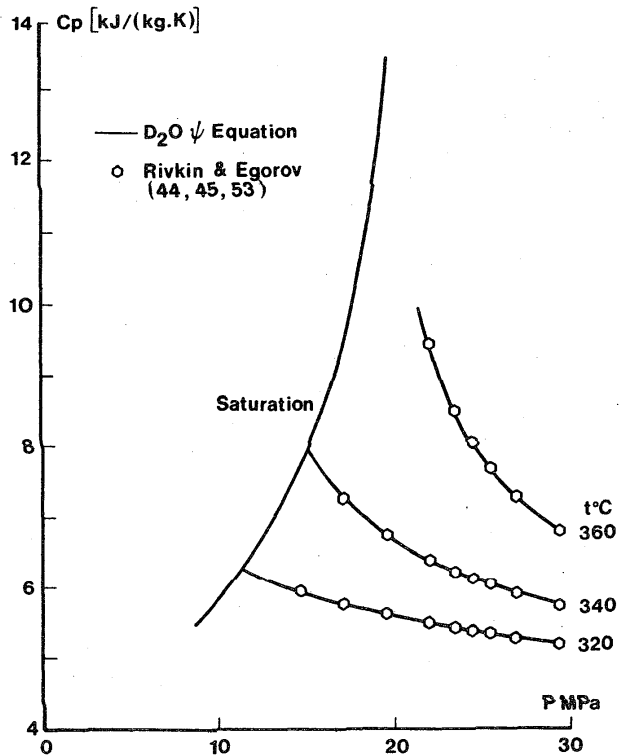


FIGURE 19. Specific heats at constant pressure: 320–360 °C.

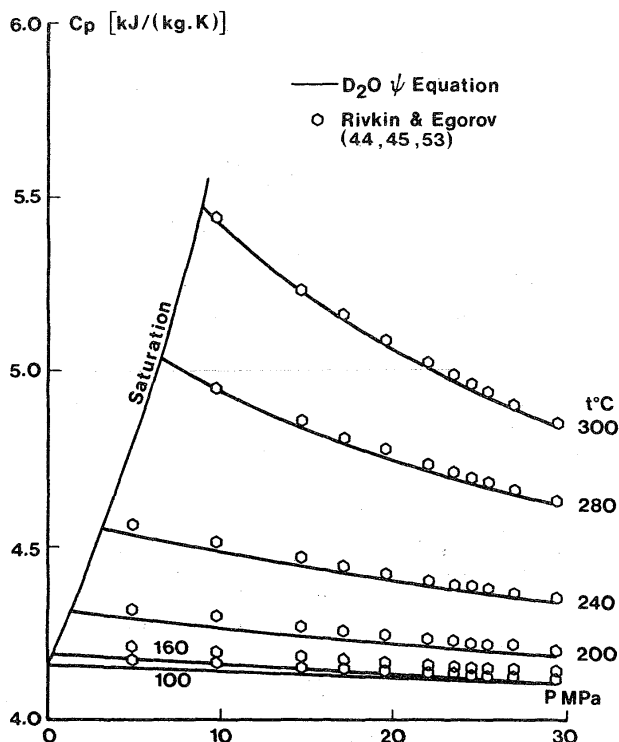


FIGURE 20. Specific heats at constant pressure: 100–300 °C.

region behaviour includes the specific heat singularity along the critical isochore:

$$C_p \sim (T_c - T)^{-\alpha}$$

where

$$\alpha \approx 0.1.$$

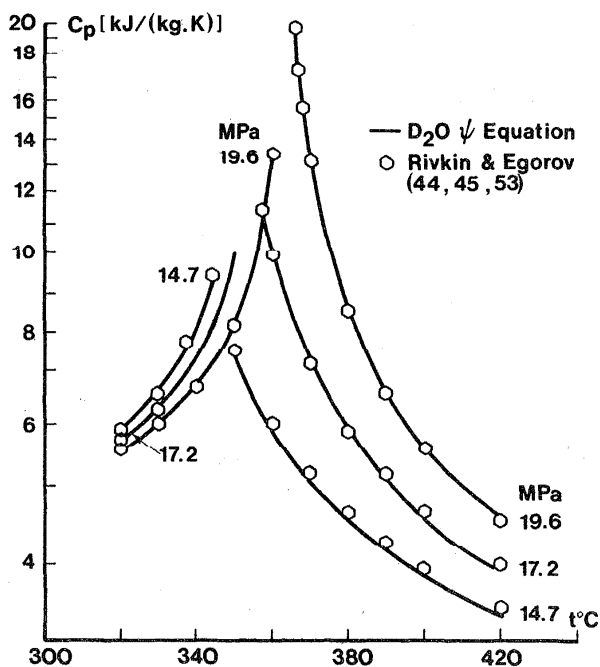


FIGURE 21. Specific heats at constant pressure: 14.7, 17.2, 19.6 MPa.

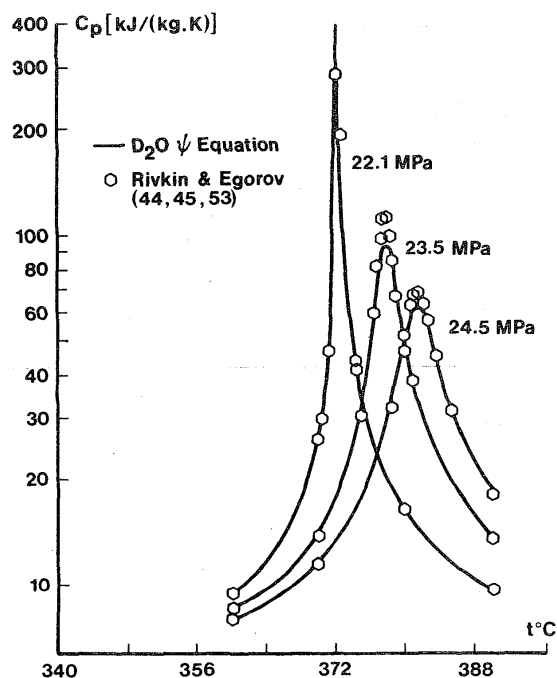


FIGURE 22. Specific heats at constant pressure: 22.1, 23.5, 24.5 MPa.

7.6. Speed of Sound

Figure 26 indicates the agreement between the D_2O speed of sound measurements of Wilson [54] and Alexandrov and Larkin [55], and the calculated values. The values agree within 2 m/s, except at 97 MPa, where the difference is up to 10 m/s, and at 0.1 MPa, where the difference is up to 6 m/s. Alexandrov's measurements have been corrected for H_2O impurity, while the measurements of Wilson have not. However, for Wilson's data, the correction would be only of the order of about 0.2 m/s for 99.8% D_2O (see Wilson [54] and Mathieson and Conway [56]).

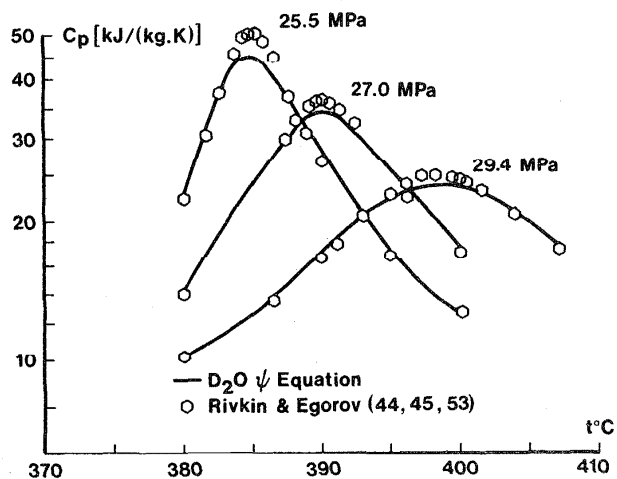


FIGURE 23. Specific heats at constant pressure: 25.5, 27.0, 29.4 MPa.

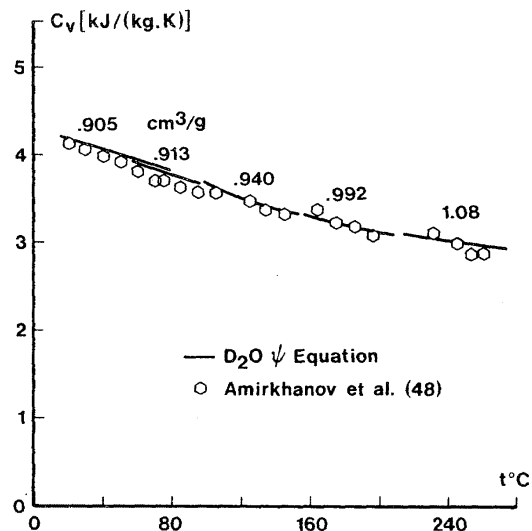


FIGURE 24. Specific heats at constant volume: 0.9–1.1 cm³/g.

Figure 27 shows a comparison of the calculated and experimental values of the speed of sound provided by Alexandrov and Larkin [55] for the temperature range 150–371 °C.

7.7. Joule-Thomson Coefficient

Figure 28 compares observed and calculated Joule-Thomson coefficients. The calculated values differ from the limited experimental data of Juza, Kmonicek, Sifner and Schovanec. The apparent disagreement in the effect of temperature on μ_J is of the same order of magnitude as the Ertle correction of the

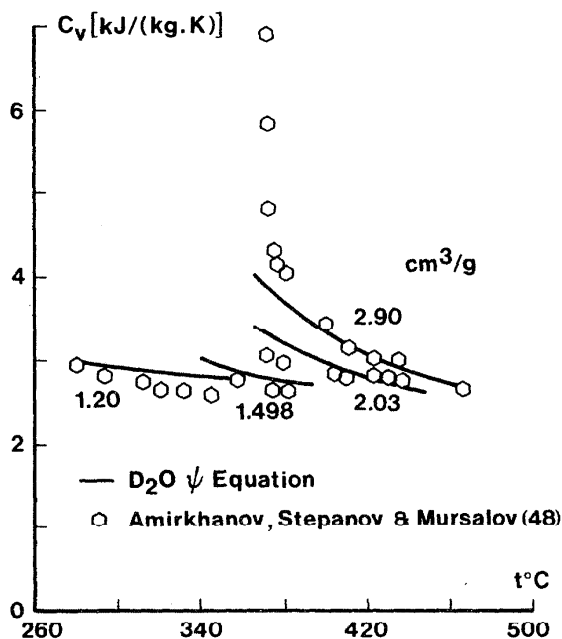


FIGURE 25. Specific heats at constant volume: 1.2–2.9 cm³/g.

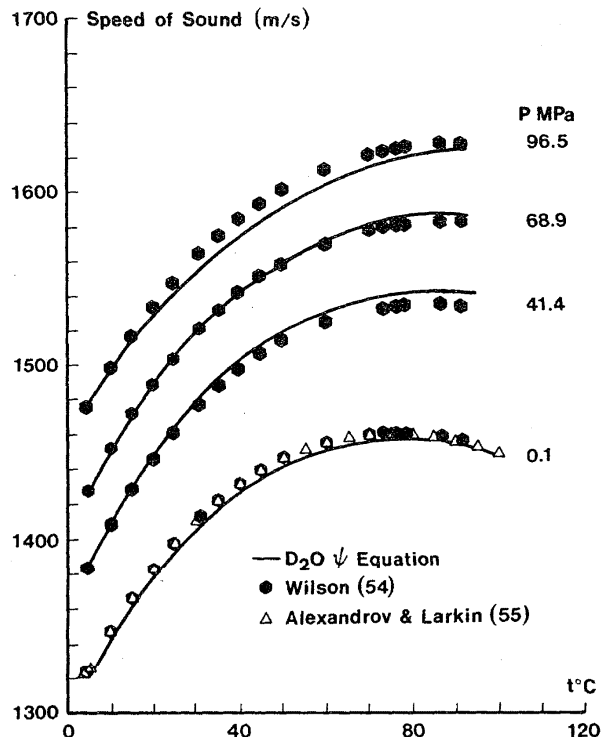


FIGURE 26. Speed of sound: comparison of values, 0–100 °C.

corresponding Juza data for H₂O [26]; Ertle uses the method of Hoxton. Thus, the discrepancy may be within the experimental uncertainty.

8. Conclusion

A fundamental equation of state has been developed for D₂O for the whole field of liquid and vapor states from the triple

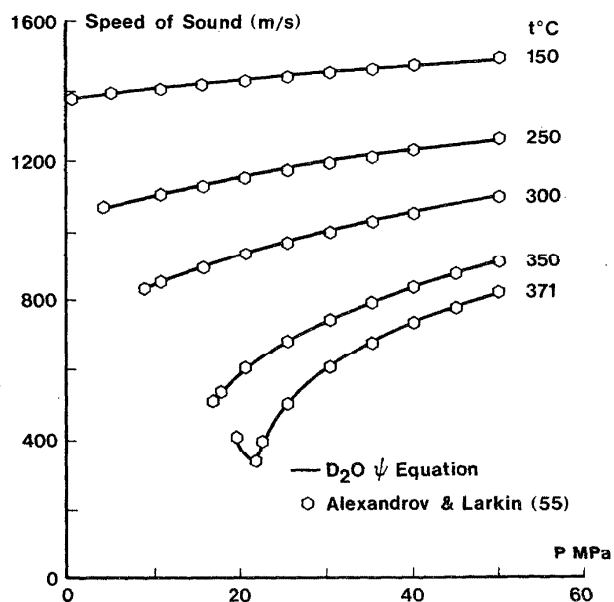


FIGURE 27. Speed of sound: comparison of values, 150–371 °C.

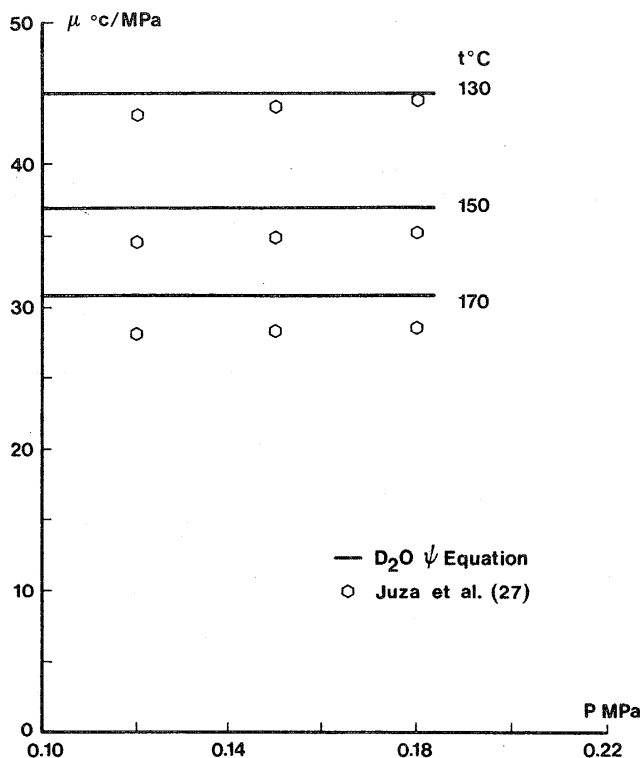


FIGURE 28. Joule Thomson coefficients: comparison of values, 130–170 °C.

point up to 600 °C and 100 MPa. *PVT*, specific heat, and speed of sound data are generally represented within the accuracy of the data, except possibly very close to the critical point and at maximum pressure and temperature where data are scarce. The equation is in agreement with a new formulation of the vapor pressure of D_2O within 0.01% except very close to the critical point, where it is still within experimental uncertainty.

Acknowledgment

This work has been supported jointly by the Atomic Energy of Canada Limited, and the Ontario Hydroelectric Power Corporation. The authors are grateful for the generous cooperation of Dr. George Kell in supplying us with unpublished data, and for many hours of helpful discussion. They are also much indebted to members of Working Group 1 (Equilibrium properties) of the International Association on the Properties of Steam for their helpful criticism on a number of occasions.

References

- [1] Keenan, J. H., Keyes, F. G., Hill, P. G., and Moore, J. G., *Steam Tables*, John Wiley and Sons, Inc., New York (1969).
- [2] Pollak, R., "The Thermodynamic Properties of Water Up to 1200 K and 3000 Bar," Doctoral Dissertation, Bochum (1974). English translation IUPAC Thermodynamics Tables Project, Dept. Chem. Eng. and Chem. Technology, Imperial College of Science and Technology London (1976).
- [3] Kirschenbaum, I., *Physical Properties and Analysis of Heavy Water*, McGraw-Hill, New York (1951).

- [4] Kesselman, P. M., "The Equation of State for Liquid Heavy Water," *Teplotenergetika* 7, (4), 72 (1960).
- [5] Baker, B. L., "Heat Capacity and Thermodynamic Properties of Saturated Deuterium Oxide," AECU-4738, U.S. Atomic Energy Commission (1959).
- [6] Mamedov, A. M., "The Equation of State for Heavy Water According to Experimentally Determined *p-V-T*," *Teplotenergetika* 7, (9), 71 (1960).
- [7] Plank, R., B. W. K. 13, 257 (1961).
- [8] Suvorov, N. P., *Zhur. Fiz. Khim.* 36, 216 (1962).
- [9] Elliot, J. N., "Tables of the Thermodynamic Properties of Heavy Water," AECL-1673, Atomic Energy of Canada, Chalk River, Ontario (1963).
- [10] Kirillin, V. A. (ed), *Heavy Water Thermophysical Properties*, Israel Program for Scientific Translations Ltd. Available from U.S. Department of Commerce National Technical Information Service, Springfield, V.A. 22151, translation (1971).
- [11] Lundquist, B., and Persson, T., B.W.K. 17, 356 (1965).
- [12] Rosta, P. Z., "Specific Heat and Enthalpy of Liquid Heavy Water," AECL-3689 Atomic Energy of Canada Limited, Power Projects, Sheridan Park, Ontario (1971).
- [13] Ivey, C. M., and Tarasuk, J. D., *Trans. A.S.M.E.* 93-C, 465 (1971).
- [14] Scheffler, K., Nitsche, W., Straub, J., P,V,T-Zustandsgrossen Von Scherem Wasser," Technische Universitat, Munich (1976).
- [15] Ikeda, M., Kageyama, Y., and Nagashima, A., "Equation of State for D_2O in the Liquid Region of up to 1000 Bar," *Bulletin JSME* 20, 1492 (1977).
- [16] Juza, J., and Mares, R., "Equation of State for Saturated and Superheated Steam D_2O up to 500 °C," *Acta Technica Csav* 23, 1 (1978).
- [17] Uematsu, M., and Watanabe, K., "Survey of the Thermophysical Properties of Heavy Water (D_2O)," Submitted to the Meeting of Working Group I of the International Association of the Properties of Steam, Ottawa, Canada, September (1975).
- [18] Hill, P. G., and MacMillan, R. D. C., "A Saturation Vapor Pressure Equation for Heavy Water," *Ind. Eng. Chem. Fundam.* 18, 412 (1979).
- [19] Hill, P. G., and MacMillan, R. D. C., "Saturation States of Heavy Water," *J. Phys. Chem. Ref. Data* 9, 735 (1980).
- [20] McCarty, R. D., "Determination of Thermodynamic Properties," Chapter 10 in *Experimental Thermodynamics*; Vol. II of *Experimental Thermodynamics of Non Reacting Fluids*, B. Le Neindre and B. Vodar, eds., Butterworths, London (1975) and Pergamon Press.
- [21] Kell, G. S., "Effects of Isotopic Composition, Temperature, Pressure and Dissolved Gases on the Density of Liquid Water," *J. Phys. Chem. Ref. Data* 6, 1109 (1977).
- [22] Whalley, E., "The Thermodynamic and Transport Properties of Heavy Water," *Proc. Conf. Thermo. and Transport Properties of Fluids*, I. Mech. E., pp. 15–26 (1957).
- [23] Friedman, Abraham S., and Haar, Lester, "High Speed Machine Computation of Ideal Gas Thermodynamic Functions I. Isotopic Water Molecules," *J. Chem. Phys.* 22, 12, pp. 2051–2058 (1954).
- [24] Kell, G. S., McLaurin, E. E., and Whalley, E., "*PvT* Properties of Water III. Virial Coefficients of D_2O ," *J. Chem. Phys.* 49, 2839 (1968).
- [25] Kell, G. S., Unpublished except for certain data presented in McLaurin, G. E. and Kell, G. S., "The Density of the Vapour of Light and Heavy Water Near Saturation in the Range 150 to 350 °C," *Proc. 9th Int. Conf. on Properties of Steam*, Munich, September 10–14 (1979).
- [26] Hill, P. G., "Virial Equations for Light and Heavy Water," to be published.
- [27] Juza, J., Kmonicek, V., Sifner, O., and Schovanec, K., "A Contribution to the Problem of Thermodynamic Similarity of H_2O and D_2O ," *Physica* 32, 362 (1966).
- [28] Tanishita, I., Watanabe, M., Uematsu, M., and Eguchi, K., "Evaluation and Correlation of Saturation Pressure of Light and Heavy Water," *Proc. 8th Int. Conf. on the Properties of Water and Steam*, Giens, France, September (1976).
- [29] Wagner, W., "A New Correlation Method for Thermodynamic Data Applied to the Vapour Pressure Curve of Argon, Nitrogen and Water," IUPAC Thermodynamic Tables Project Centre, Dept. Chem. Eng. and Chem. Tech., London (1977).
- [30] Blank, G., "A New Determination of the Critical Point of Light and Heavy Water," (in German), *Warme and Stoffubertragung* 2, 53 (1968).
- [31] Rivkin, S. L., and Ahkundov, T. S., *Teplotenergetika* 9, 5, 62 (1962).
- [32] Tsederberg, N. V., Alexandrov, A. A., and Khasanshin, T. S., "An Experimental Investigation of the Specific Volumes of Heavy Water in the Temperature Range 20–200 °C at Pressures up to 1000 Bar," *Teplotenergetika* 19, 10, 65 (1972).
- [33] Tsederberg, N. V., Alexandrov, A. A., Khasanshin, T. S., and Larkin, B. K., "Experimental Investigation of the Specific Volumes of Heavy Water in the 200–425 °C Temperature Range at Pressures up to 1000 Bar," *Te-*

- ploenergetika **20**, 8, 13 (1973).
- [34] Emmet, T. R., and Millero, F. J., "Specific Volume of Deuterium Oxide from 2° to 40 °C and 0 to 1000 Bars Applied Pressure," *J. Chem. Eng. Data* **20**, 351 (1975).
- [35] Alexandrov, A. A., Khasanshin, T. S., and Larkin, D. K., "Specific Volumes of Ordinary and Heavy Water at High Pressures and Temperatures," Report to Working Group I, IAPS, April (1976).
- [36] Bridgman, P. W., *J. Chem. Phys.* **3**, 597 (1935).
- [37] Rivkin, S. L., "Experimental Study of the Density of Heavy Water," *Atomnaya Energiya* **7**, 457 (1959).
- [38] Kirillin, V. A., and Ulybin, S. A., *Teploenergetika* **8**, 4, 67 (1959).
- [39] Rivkin, S. L., and Alkundov, T. S., *Atomnaya Energiya* **14**, 6, 581 (1963).
- [40] Steckel, F., and Szapiro, S., "Physical Properties of Heavy Oxygen Water. Part I. Density and Thermal Expansion," *Trans. Faraday Soc.* **59**, 331 (1963).
- [41] Alexandrov, A. A., Khasanshin, T. S., and Larkin, D. K., *Zhur. Fiz. Chim.* **50**, 394 (1976).
- [42] Kell, G. S., "Precise Representation of Volume Properties of Water at One Atmosphere," *J. Chem. Eng. Data* **12**, 66 (1974).
- [43] Hastings, J. R., Levelt Sengers, J. M. H., and Balfour, F. W., "The Critical-Region Equation of State of Ethylene and the Effect of Small Impurities," to be published.
- [44] Rivkin, S. L., and Egorov, B. N., "Specific Heat of Heavy Water at High Temperatures and Pressures," *Atomnaya Energiya* **7**, 5, 462 (1959). English translation in *Sivit J. At. Energy* **7**, 928 (1961) and also in *J. Nuclear Energy* **14**, 213, 137 (1961).
- [45] Rivkin, S. L., and Egorov, B. N., "Experimental Investigation of the Specific Heat of Heavy Water at High Pressure and Temperatures," *Teploenergetika* **10**, 7, 75 (1963).
- [46] Cockett, A. H., and Ferguson, A. F., "The Specific Heat of Water and of Heavy Water," *Phil. Mag. Ser. 7*, **29**, 185 (1940).
- [47] Eucken, A. and Eigen, M., *Z. Electrochemie und Phys. Chemie* **55**, 343 (1951).
- [48] Amirkhanov, Kh. I., Stepanov, G. V., and Mursalov, B. A., "An Experimental Investigation of the Isochoric Specific Heat of Heavy Water at Temperatures of 20–460 °C and Pressures up to 500 Bar," *Teploenergetika* **22**, 4, 68 (1975).
- [49] Bedford, G. S., and Kirby, C. G. M., "The International Scale of Temperature of 1968," *Metrologia* **5**, 83 (1975).
- [50] Kell, G. S., McLaurin, G. E., and Whalley, E., "*PvT* Properties of Water II. Virial Coefficients of H₂ in the Range 150°–450 °C Without Independent Measurements of Vapour Volume," *J. Chem. Phys.* **48**, 3805 (1968).
- [51] Alexandrov, A. A., Larkin, D. K., Matveev, A. B., and Ershova, Z. A., *Izvestia V. U. Z.* **11**, 84 (1977).
- [52] Alexandrov, A. A., Private Communication, August 1980.
- [53] Rivkin, S. L., and Egorov, B. N., *Teploenergetika* **9**, 12, 60 (1962).
- [54] Wilson, W., "Speed of Sound in Heavy Water as a Function of Temperature and Pressure," *J. Acoust. Soc. Am.* **33**, 314 (1961).
- [55] Alexandrov, A. A. and Larkin, D. K., *Inzhenerno-Fizicheskii Zhurnal* **34**, 110 (1978).
- [56] Mathieson, N. G. and Conway, B. E., "Ultrasonic Velocity in Water-Deuterium Oxide Mixtures," *Anal. Chem.* **44**, 1517 (1972).

Appendix A

Evaluation of C_1 and C_2

At 3.8 °C $h = h_f$ is set equal to zero (within 0.001 J/g, $h_f = u_f$ at that point).

At the same temperature it may be shown that

$$h_o = C_1 + \sum_{i=3}^6 (2-i) \left(\frac{T}{1000} \right)^{i-1} + C_7 (\ln T - 1) + \left(R - \frac{C_8}{1000} \right) T = C_1 + 457.38.$$

But one can also write

$$h_o = h_o - h_g + h_{fg} + h_f$$

or

$$C_1 + 457.38 = 0.49 + 2323.7 + 0.0.$$

Whence

$$C_1 = 1866.81.$$

The constant C_2 is obtained by setting $\psi_f = 0$ at 3.8 °C. With $u_f = 0$, this is equivalent to $s_f = 0$.

Writing

$$s_f = s_o + s_g - s_o + s_f - s_g$$

we have

$$0 = - [R \ln \rho]_{p \rightarrow 0} - \frac{d\psi_o}{dT} + \int_0^{P_{\text{sat}}} \left(\frac{\partial s}{\partial P} \right)_T dP - \frac{h_{fg}}{T}.$$

For the low temperature vapor

$$\left(\frac{\partial s}{\partial P} \right)_T = \frac{1}{T} \left(\frac{\partial h}{\partial P} \right)_T - \frac{V}{T} \approx R \frac{dB\tau}{d\tau} \left(\frac{\partial \rho}{\partial P} \right)_T - \frac{R}{P} \left(1 + \frac{B}{v} \right).$$

So

$$\int_0^{P_{\text{sat}}} \left(\frac{\partial s}{\partial P} \right)_T dP \approx \frac{R}{v_g} \frac{dB\tau}{d\tau} - R \ln P_{\text{sat}} + R [\ln P]_{p \rightarrow 0} - \frac{B}{T} P_{\text{sat}}.$$

Hence, the entropy equation becomes

$$0 = - [R \ln \rho]_{p \rightarrow 0} - \frac{d\psi_o}{dT} - R \ln P_{\text{sat}} + [R \ln P]_{p \rightarrow 0} - \frac{h_{fg}}{T} - \frac{B}{T} P_{\text{sat}} + \frac{R}{v_g} \frac{dB\tau}{d\tau}$$

which reduces to

$$C_2 = 1000 \left[-R \ln \left(\frac{P_{\text{sat}}}{RT} \right) - \frac{h_{fg}}{T} - \frac{B}{T} P_{\text{sat}} + \frac{R}{v_g} \frac{dB\tau}{d\tau} \right] - \sum_{i=3}^6 C_i (i-1) \left(\frac{T}{1000} \right)^{i-2} - C_7 \frac{1000}{T} - C_8 (\ln T + 1)$$

in which	T	= 3.8 + 273.15
	P_{sat}	= 0.00066005 MPa
	R	= 0.41515 kJ/kg·K
	h_{fg}	= 2323.7 kJ/kg
	B	≈ - .075 m ³ /kg
	$\frac{dB\tau}{d\tau}$	= - 0.4 m ³ /kg
	v_g	= 174.1 m ³ /kg.

This yields approximately

$$C_2 = 4661.5.$$